Plasma Polymerization of Ethylene in an Atmospheric Pressure-Pulsed Discharge

KEVIN G. DONOHOE* and THEODORE WYDEVEN, *Ames Research Center, NASA, Moffett Field, California 94035*

Synopsis

The polymerization of ethylene in an atmospheric pressure-pulsed discharge has been studied. Partial pressures of ethylene up to 4 kN/m^2 were used with helium as a diluent. Deposition rates (on glass slides) were the same throughout the discharge volume over a wide range of operating conditions. These rates were in the 1–2 Å/sec range. The films were clear, soft, and showed good adhesion to the glass substrates. Oligomers large enough to visibly scatter 637.8-nm light were observed in the gas phase under all conditions in which film deposition occurred. The experimental results suggest that Brownian diffusion of these oligomers was the rate-limiting step in the film deposition process.

INTRODUCTION

Applications of the technique of plasma polymerization include the production of antireflection and scratch resistant coatings for plastic optical components,[1,2] hyperfiltration membranes for water purification,[3] and protective coatings for materials such as laser windows.[4,5] Many of these techniques have been recently reviewed.[6] At the present time, most reported plasma processes are carried out at low pressures—of the order of 300 N/m^2 or less. This report describes the experimental characterization of a plasma polymerization reactor which operates at atmospheric pressure (101 kN/m^2).[7,8] The interest in operating at this pressure was based on the economic advantages of operating a plasma system without the need for vacuum equipment or batch processing. In addition, it was anticipated that operation of a discharge at a high partial pressure of monomer might result in a high deposition rate of polymer films. Ethylene was chosen as a monomer because ethylene polymerization has been studied in considerable detail in low-pressure radio-frequency glow discharges.[9,10]

EXPERIMENTAL

Discharge Circuit

The electric discharge circuit and plasma reactor are shown in Figure 1. The circuit consists of a high-voltage 60-Hz power supply which charges the capacitors C in an LC resonant circuit to a voltage determined by the spark gap electrode separation. When the spark gap fires, the circuit resonates with a frequency of approximately $1/\sqrt{LC}$. This oscillation excites the secondary of the Tesla transformer and results in the production of a large amplitude (up to 80 kV) ac

* National Research Council Research Associate.

Journal of Applied Polymer Science, Vol. 23, 2591–2601 (1979)

0021-8995/79/0023-2591$01.00

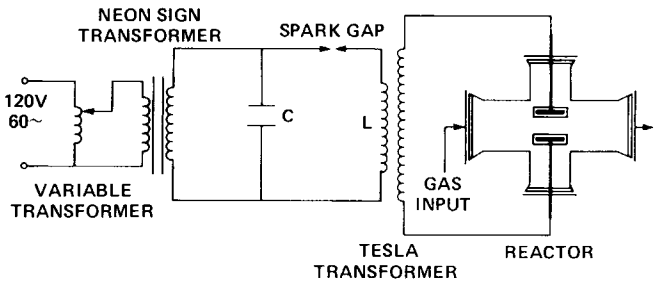

Fig. 1. Schematic of the discharge circuit and the reactor.

voltage across the electrodes in the reactor. The rate at which the spark gap fires is controlled by the setting of the variable transformer. The capacitors used for the experiments described here were 5000 pF ceramic doorknob capacitors (Sprague Electric Co., North Adams, Mass.). The Tesla transformer primary consisted of six turns of 0.32-cm-diameter copper tubing. This coil was 20 cm in diameter and 20 cm long. The secondary was 636 turns of No. 30 cotton-covered wire wound on a 7.6-cm-o.d. phenolic tube. Further details of the circuit construction and operation are given in ref. 7. The waveforms associated with the operation of the circuit are shown in Figure 2.

The waveform in Figure 2(a) shows the spark gap voltage with a spark gap firing rate of 120 sec^{-1}. At a firing rate of 480 sec^{-1} (the rate used for most of the measurements described here), the gap fired four times during each half-cycle of the 60-Hz applied voltage. The waveform in Figure 2(b) is the no-load applied voltage. This represents the output voltage of the Tesla transformer. Due to the nature of the breakdown of the spark gap, the amplitude of the first half-wave is smaller than that of the second half-wave.[7] The waveforms in Figure 2(c) illustrate the breakdown waveforms. Because of the symmetry of the circuit and the electrodes, the breakdown waveform is independent of the polarity of the pulsed discharge. The breakdown waveforms show two characteristics: a "breakdown" voltage, V_b and an extinction voltage V_e. The breakdown voltage V_b is the voltage at which the circuit begins to load down due to current flow through the plasma and V_e is the voltage at which the discharge turns off. The current takes the form of a pulse which begins when the voltage reaches V_b and ends when the voltage reaches V_e. The time duration of the current is of the order of 100 nsec, and the rise time of the current pulse is nearly equal to its fall time.

Reactor Geometry

The reactor (Fig. 1) consists of a glass pipe cross (Corning Glass Works, Corning, N.Y.) with a 15.2–cm i.d. in the direction of gas flow and a 10.1-cm i.d. along the electrode axis. The cross was sealed with stainless steel end plates on the sides and poly(methyl methacrylate) end plates on the top and bottom. These dielectric end plates were necessary to isolate the electrodes from the metal rack that supported the reactor and to reduce corona losses.

The electrodes were brass disks 9.5 cm in diameter and 1.25 cm thick with edges of 0.16-cm radii. The electrodes were potted in polyester casting resin (Al Paint and Varnish Co., Torrance, Calif.) and then machined to a 11.4-cm diameter with

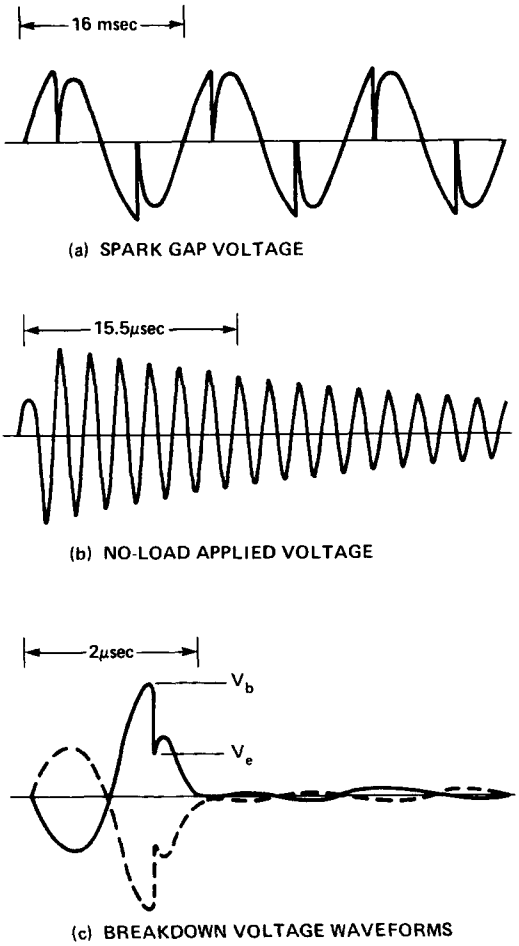

Fig. 2. Oscillograms of the voltage waveforms of the discharge circuit.

a 0.318-cm-thick polyester coating on each electrode face. This electrode design permits the production of a volumetric discharge by limiting, but not preventing, secondary cathode emission.[7] Secondary emission could still occur at the joint between the resin and the 0.95-cm-diameter stem at the back of each electrode. In the work leading to the results discussed below, an electrode gap of 3.81 cm was used.

Diagnostics

The potential difference between the electrodes was measured with two Tektronix P6015 high-voltage probes. Two probes were needed because the Tesla transformer secondary floats with respect to ground. The probe signals were subtracted from each other with the oscilloscope amplifier. A Tektronix 5403 oscilloscope with 5A48 amplifiers and a 5B42 time base was used. The current was measured with a Pearson 4100 current probe.

Gas-chromatographic analysis of the plasma gas was accomplished using a Carle Model 100 gas chromatograph (Carle Instruments, Fullerton, Calif.) with

a thermal conductivity detector. A 1.5-m Porapak Q/T column was used to separate the hydrocarbons. The detector was calibrated with an exponential dilution chamber.[11] The sampling probe was a 0.1-cm-i.d. glass tube mounted in a nylon ball joint in the downstream end plate. The tube end could be located anywhere in the plasma volume by moving the ball joint and by sliding the tube in and out. The gas samples were drawn through the tube into the sampling valve of the chromatograph. The sampling probe had no effect on the visual or measured electrical properties of the plasma and its presence had no effect on the deposition rate. The spatial resolution of the probe was calculated by setting the ratio of its volumetric sampling rate to the average gas velocity in the reactor equal to the area of a circle. The diameter of a circle encompassing this area was taken as the spatial resolution of the probe. For example, for the 8.8-cm^3/sec flow rate data discussed below and a gas sampling rate of 0.04 cm^3/sec, the spatial resolution was 0.7 cm.

Film thicknesses were measured by depositing films on masked glass slides and measuring the resulting step height with a Sloan M-100 angstrometer or Taylor Hobson Model 3 Tallysurf surface profilometer.

RESULTS

Operation of a uniform glow discharge in pure ethylene was not possible at atmospheric pressure. With the electrode configuration used here, a discharge in pure ethylene constricted at pressures in excess of 4 kN/m^2. Consequently, helium was used as a diluent to raise the pressure to 1 atm (101 kN/m^2). With helium as a diluent, a uniform discharge could be maintained at a partial pressure of ethylene of 8 kN/m^2. Thus the presence of the helium permitted the partial pressure of ethylene to be doubled before the discharge became constricted. This increase in the maximum partial pressure of ethylene is due in part to the high thermal conductivity of helium and to the fact that constriction under these conditions is thermal in nature.[7,12]

Films were deposited on glass microscope slides which were oriented parallel to the electrode faces. Within experimental error, deposition rates were independent of vertical position in the discharge and were the same on the lower and upper surfaces of the glass slides. Unless otherwise noted, all of the results discussed below were obtained under conditions in which the deposited films were of uniform thickness.

In all cases, the films were uncolored and not the characteristic straw yellow color often observed for plasma-polymerized films. The films were soluble in ethanol, suggesting that they were not highly crosslinked. Freshly prepared films had an olefinic odor (similar to ethylene) which disappeared after a few weeks of storage in room air. The polymerized material formed films rather than oils, and small chunks of flexible, opaque white polymer could be scraped from the glass slides. The films passed the cellophane tape pull test (Mil Spec M-13508C) for adhesion to the glass substrate. The softness of the film was evidenced by the scratches produced when the films were lightly brushed with a camel's hair brush.

Infrared transmission spectra of the ethylene films deposited on cesium iodide windows showed no absorption around 1600 cm^{-1}, indicating the absence of significant amounts of vinyl groups or unsaturation in the polymer film. In

general, the IR spectra were similar to those of ethylene films produced in a low-pressure radio-frequency glow discharge.[13]

Elemental analysis of a typical film yielded the following empirical formula: $C_2H_{3.26}O_{0.23}$. Typical literature values[9] for n in C_2H_n are in the range of 2.6–3 for rf discharge-produced ethylene films, while for linear conventional polyethylene, $n = 4$. The lower degree of hydrogen abstraction observed here ($n = 3.26$) suggests that less branching or crosslinking is present in the polymer films produced here than in films produced at lower pressure in an rf discharge.

An important difference between polymerization in this atmospheric pressure-pulsed discharge and in low-pressure rf discharges[10] is that in the high-pressure discharge, oligomers large enough to visibly scatter light from a He–Ne laser (632.8 nm) were always observed in the gas phase. Under conditions in which uniform clear films were produced, these scattering centers were uniformly distributed throughout the discharge volume. Qualitatively, their gas-phase density (estimated by observing the intensity of the scattered laser radiation) was highest under conditions of highest rates of deposition (up to 3 Å/sec). However, the films produced at these high rates were not clear; the films were fogged and almost opaque. It has been noted that in low-pressure discharges, high deposition rates are also accompanied by powder formation and the production of opaque films.[14] Fogging of films can be due to surface roughness or to the presence of scattering centers embedded in the bulk film. A prior scanning electron microscope (SEM) study of particle incorporation in plasma-polymerized organosilicon films[15] showed that submicrometer-diameter spheres were uniformly distributed throughout the polymer films. However, no such particles were observed with the films produced here (25 nm resolution). Thus, the fogged appearance of the films produced here was apparently due to surface roughness and not to the presence of particles embedded in the bulk film.

The magnitude of the surface roughness required to cause fogging can be estimated. One criterion[16] states that diffuse reflectance begins when the roughness height h is greater than $\lambda/16$ for normal incidence of light of wavelength λ. For visible light (400–700 nm), this corresponds to h between 25 and 44 nm. SEM examination of a fogged film surface revealed the presence of rounded particles on the film surface (Fig. 3). This SEM photograph was taken with the sample at an angle of 45° relative to the electron beam. Particles with diameters of 800 to 5000 nm (0.8–5 μm) are evident in the figure, and they appear to protrude from the surface by 400–2500 nm. It is evident from Figure 3 that the larger particles are agglomerates of smaller particles. Similar SEM examination of a clear film showed absolutely no structure (25 nm resolution). So, under conditions in which clear films are deposited, the gas-phase oligomers could be either too small to produce diffuse reflectance on the surface (smaller than 25 nm) or they could incorporate homogeneously into the bulk polymer film.

Discharge Power

The work done by the circuit during a single discharge is equal to the time integral of the instantaneous power of a single discharge. The power is the vector dot product of the voltage (Fig. 2) and the current. The peak instantaneous power delivered by the circuit is given by the expression $[V_e + (V_b - V_e)/2]i_p$, where V_b and V_e are the voltages shown in Figure 2 and i_p is the peak current.

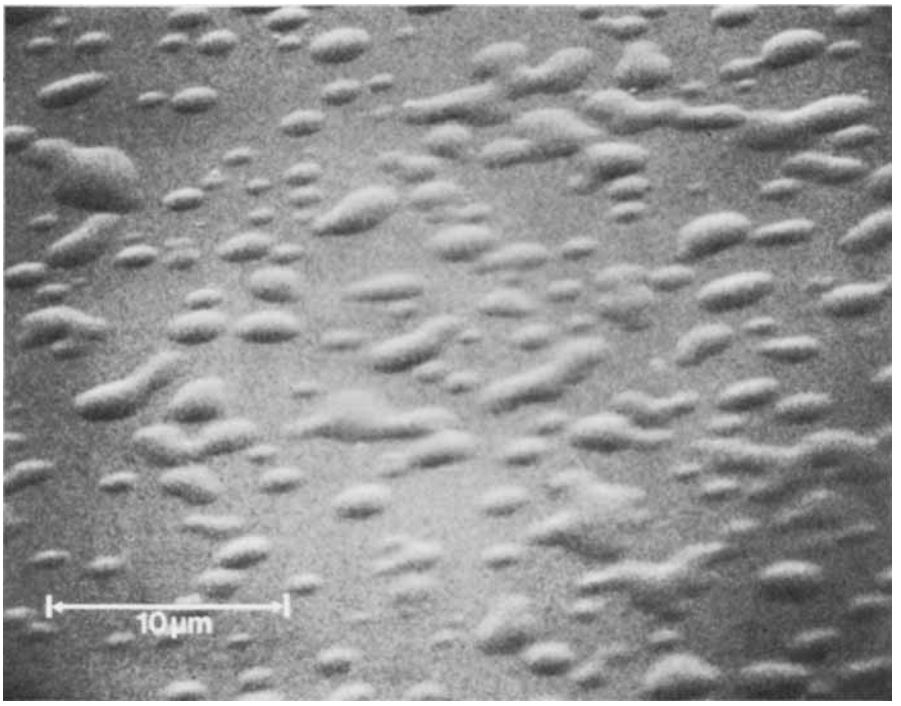

Fig. 3. SEM photograph of a fogged film with the sample at an angle of 45° relative to the electron beam.

For the conditions discussed below, the peak discharge power was 22 kW, and the average power (firing rate = 480 sec^{-1}) was 0.5 W. These were calculated from the following values: $V_b = 20$ kV, $V_e = 9$ kV, $i_p = 1.5$ A. The time duration of the nearly symmetrical current pulse was 100 nsec.

The values of the peak and average discharge power given above are maximum values because losses in the dielectric coatings of the electrodes were neglected. The voltage drop across the dielectric faces must be known if the actual power delivered to the gas is to be calculated. Because an unknown fraction of the total current is displaced through the dielectrics (the rest of the current flows from the back of the electrodes where secondary production of electrons occurs), the actual voltage drop across these dielectrics cannot be calculated exactly. It can be estimated if the fraction of the total current which is displaced is known. For an atmospheric pressure discharge in pure helium using similar (but not identical) electrodes, the percentage of the total current that was displaced through the dielectrics was estimated[7] to be 20%. A lower bound on the discharge power can be obtained if it is assumed that all of the current is displaced through the dielectric coatings.

If it is assumed that all of the current is displaced through the dielectrics, then the relationship between the displacement current i and the time rate of change of voltage across the dielectrics is

$$i = \frac{AK\epsilon_0}{d}\frac{dV}{dt} \simeq \frac{Ak\epsilon_0}{d}\frac{\Delta V}{\Delta t}$$

where A is the cross section available for current flow, d is the thickness of the

dielectric, ϵ_0 is the permittivity of free space, and K is the dielectric constant of the material. For a 1.5-A current pulse with a 50-nsec rise time, the voltage drop (ΔV) across each dielectric face is 2.5 kV ($K = 3$). This gives a minimum peak power of 14.25 kW and a minimum average power of 0.34 W. This value for the average power is considerably smaller than those used in low-pressure rf discharges of comparable reactor volume.[3,6]

Spark Gap Firing Rate

The power in a pulsed discharge can be varied in two ways: the power per pulse can be varied or the pulse repetition rate can be varied. With the circuit used here, the power per pulse can be varied by the magnitude of the spark gap electrode separation. In addition, the spark gap firing rate can be varied by changing the output of the variable transformer (Fig. 1). Since the voltages and current did not vary significantly as the firing rate was varied from 60 to 840 sec^{-1}, the power per pulse was essentially constant, and therefore the average power varied directly with the firing rate. In Figure 4, the film deposition rate is seen to vary linearly with the spark gap firing rate for rates up to 600 sec^{-1}. This finding suggested that the same amount of polymer was formed each time a discharge occurred. For rates higher than 600 sec^{-1}, the deposition rate did not increase linearly with firing rate. This indicated that either a change in the mechanism or mechanisms of polymer deposition occurred or that a nonlinear relationship existed between the production of active species and the firing rate. The low average power (about 1 W at 960 sec^{-1}) suggests that temperature changes were not responsible for the nonlinear relationship between firing rate and deposition rate.

The ethylene concentration was measured at various locations inside the plasma with the sampling probe described earlier. The measurements indicated that the ethylene concentration was constant in the direction parallel to the

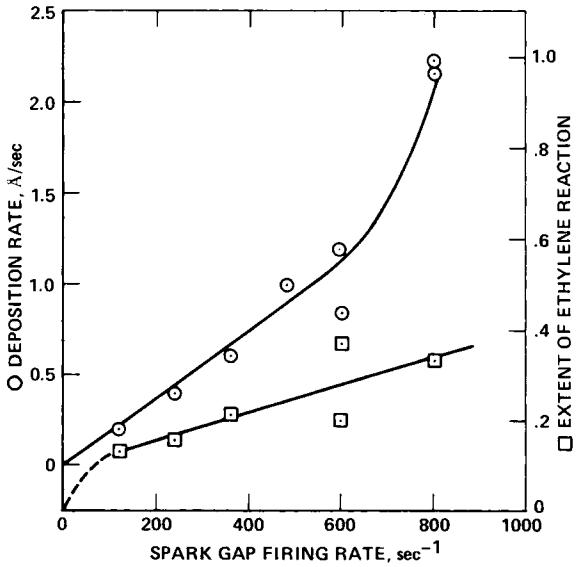

Fig. 4. Film deposition rate (⊙) and extent of ethylene reaction (⊡) vs spark gap firing rate.

electric field and that its concentration decreased nearly linearly in the direction parallel to the monomer flow for the flow rates used in this work. Therefore, ethylene concentrations c were monitored in the center of the reactor, and $(c_0 - c)/c_0$ was proportional to the extent of reaction of ethylene. The variation of $(c_0 - c)/c_0$ and the deposition rates with the spark gap firing rates are shown in Figure 4. In this figure, the extent of ethylene reaction varies linearly with the firing rate, even at the high rates that produced a nonlinear change in the deposition rate. Hence, the deposition rate did not vary directly with the amount of ethylene consumed.

Gas Flow Rate

The effect of gas flow rate on the polymer deposition rate is shown in Figure 5(a) for two different ethylene feed concentrations. The range of flow rates in Figure 5 corresponds to mean residence times from 60 sec (16.6 cm^3/sec flow rate) to 1290 sec (0.83 cm^3/sec flow rate). All of the flow rates reported here are at NPT. The characteristic time for diffusion of ethylene across the discharge zone is 7 sec. Therefore, the reactor was operated in a flow rate regime in which diffusion was fast compared to convection. The abscissa in Figure 5 represents the total flow rate into the reaction chamber and includes that portion of the feed (about 30%) which bypassed the plasma. The deposition rate is seen to be virtually independent of the flow rate for flows in excess of 5 cm^3/sec. Below 5

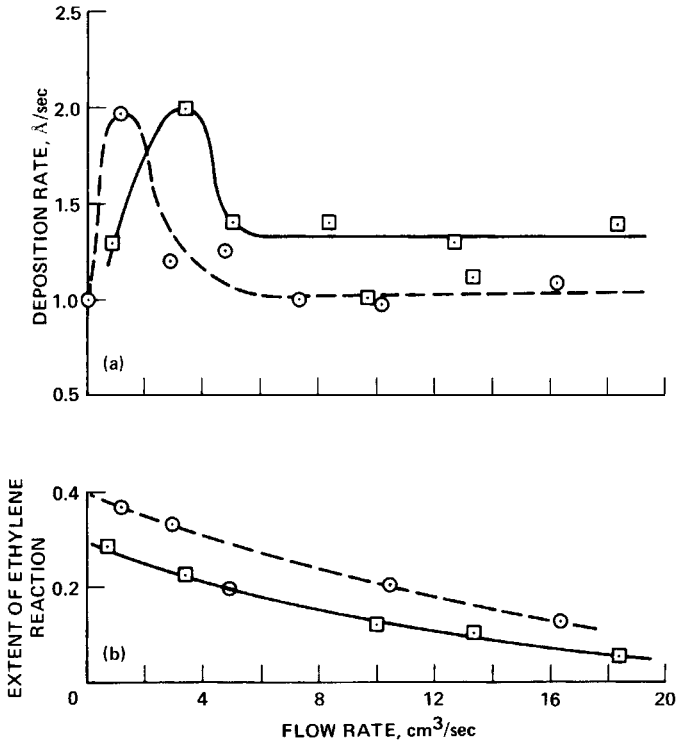

Fig. 5. Film deposition rate and extent of ethylene reaction vs gas flow rate (NPT): (⊙) 1% C_2H_4 in feed; (⊡) 2% C_2H_4 in feed. Firing rate 480 sec^{-1}.

cm^3/sec the rate increases to a maximum and then decreases. At very low flow rates the deposition rate is limited by the supply of monomer. As the flow rate is increased, a point is reached at which the gas residence time becomes insufficient for large gas-phase free-radical concentrations to be attained, and consequently the deposition rate declines as the flow rate is further increased. The plateau in deposition rate suggests that at high monomer flow rates, deposition is controlled *not* by gas-phase processes but rather by processes occurring at the plasma–substrate interface. Thus, in this limit the free radicals necessary for polymer formation might be formed via the impact of ions and electrons with the growing polymer film. It is therefore quite likely that deposition is controlled by radical formation both at the surface and in the gas phase for low monomer flow rates and at the surface alone for high monomer flow rates.

The variation of the extent of ethylene reaction with flow rate is shown in Figure 5(b). Although it is not evident from the figure, the extent of reaction was directly proportional to the reciprocal of the flow rate for flow rates greater than 5 cm^3/sec. This means that each time the discharge occurred, the same amount of ethylene was reacted.

Ethylene Feed Concentration

The feed concentration of ethylene was varied from 0.2 to 3.7 vol-% for different flow rates between 3.7 and 8.3 cm^3/sec. A spark gap electrode separation of 0.076 cm was used with a firing rate of 480 sec^{-1}. The deposition rate was independent of flow rate and varied by less than a factor of 2 with ethylene concentration. The rate increased with increasing ethylene feed concentration.

Gaseous Discharge Products

Gas-chromatographic analyses of the gas in the discharge showed that acetylene was the major volatile product of the ethylene discharge. Ethane was also produced but in a much lower concentration than acetylene: the ratio of ethane to acetylene concentration was typically in the 0.02–0.07 range. No other gaseous products were observed (within the detection limits of the chromatograph). These results are similar to those obtained by others[9] in a mass-spectrometric analysis of the effluent from a low-pressure rf discharge in ethylene. The limits of detection of the chromatograph used here were evaluated for butane and heptane and were 50 and 200 ppm, respectively.

DISCUSSION

The most obvious difference between films that were produced under different conditions in this work was their surface morphology. Because light-scattering oligomers were always observed in the gas phase when film deposition occurred, it is likely that the observed micrometer-sized particles in the fogged film surfaces were individual oligomers or aggregates of oligomers. The difference between the oligomers which form when fogged or clear films were deposited is likely to have been the size to which they grow in the gas phase before reaching the growing film surface. It is also possible that they differed chemically and that the oligomers present under conditions in which fogged films were formed were not

reactive enough to form a smooth surface. In both cases the oligomers may have been oils or polyradicals.

The following discussion includes a description of the motion of these oligomers in the gas phase and a description of the proposed gas-phase chemical reactions.

Chemical Reactions in the Gas Phase

Chromatographic analysis of the gas in the discharge showed that the rate of disappearance of ethylene did not vary directly with the film deposition rate. Chromatographic analysis also revealed that acetylene was the principal gaseous product of the ethylene–helium discharge and that only traces of higher molecular weight hydrocarbons were present. The appearance of acetylene is consistent with a free-radical mechanism for polymerization similar to the one proposed[9] to describe the low-pressure polymerization of ethylene in an rf discharge:

Initiation

$$e^- + C_2H_4 \rightarrow C_2H_2 + 2H\cdot + e^- \quad (1)$$

$$e^- + C_2H_4 \rightarrow C_2H_2 + H_2 + e^- \quad (2)$$

Propagation

$$H\cdot + C_2H_4 \xrightarrow{(M)} C_2H_5\cdot \quad (3)$$

$$C_2H_5\cdot + C_2H_4 \rightarrow C_4H_9\cdot \quad (4)$$

$$(C_nH_{2n+1})\cdot + C_2H_4 \rightarrow (C_{n'}H_{2n'+1})\cdot \quad (5)$$

Termination

$$(C_nH_{2n+1})\cdot + R\cdot \rightarrow \text{stable products} \quad (6)$$

Oligomer Motion in the Gas Phase

The observation that the film deposition rate was nearly independent of feed concentration, flow rate, and extent of ethylene reaction over wide ranges of these variables suggested that some mass transfer process limited the deposition rate. Therefore, an attempt was made to relate the motion of the oligomers in the gas phase to the observed deposition rates.

The motion of micrometer- and submicrometer-sized particles in the gas phase can be due to convection, Brownian motion, and sedimentation. Convection occurred perpendicular to the direction of the mass flux that produces deposition and was considered unimportant under conditions of uniform deposition. In helium at NPT, the Brownian displacement of a particle in 1 sec equals the sedimentation displacement for particles of the order of 500 nm in diameter and unit density.[17] For particles smaller than 500 nm in diameter, Brownian motion dominates sedimentation. This can explain why the deposition rate of clear films was observed to be the same on the top and bottom of glass cover slips positioned between the electrodes.

It is of interest to note that limited agglomeration of the oligomers would have a relatively small effect on the Brownian motion of the agglomerates because the Brownian diffusion coefficient varies with the reciprocal of the particle radius. For example, a twofold increase in the particle radius requires an eightfold increase in its mass. This means that eight particles would have to combine to decrease the Brownian diffusion rate by a factor of 2. This relatively insensitive response of the diffusion coefficient to agglomeration is a likely explanation for the fact that the deposition rate is independent of gas flow rate over such a large range of flow rates.

SUMMARY AND CONCLUSIONS

Plasma polymerization of ethylene has been studied in a pulsed electrical discharge which operated at atmospheric pressure. Films produced in this discharge were soft, uncolored, soluble in ethanol, and passed the cellophane tape pull test for adhesion to a glass substrate. These observations, coupled with the infrared spectra and elemental analysis of the polymer, indicated that the degree of unsaturation and/or crosslinking was low. The low degree of hydrogen abstraction and lack of crosslinking is consistent with the low average electron energies (due to the low electric field-to-pressure ratio) present in the high-pressure discharge.

A free-radical chain reaction scheme to explain the polymerization is consistent with the results obtained in this work. Gas-chromatographic analysis of the gas in the plasma revealed that acetylene was the principal gaseous product of the ethylene–helium discharge and that only traces of higher molecular weight hydrocarbons were present. Brownian diffusion of the oligomers formed in the gas phase was suggested to be the rate-limiting step in the film deposition process under the conditions of constant firing rate and low duty cycle.

The authors thank John Banks for his assistance in helping set up the gas-chromatographic analysis system used in this work, and also Dr. E. V. Ballou for his many helpful suggestions and comments concerning the manuscript.

References

1. T. Wydeven, *Appl. Opt.*, **16**(3), 717 (1977).
2. T. Wydeven and R. Kubacki, *Appl. Opt.*, **15**(1), 132 (1976).
3. A. T. Bell, T. Wydeven, and C. Johnson, *J. Appl. Polym. Sci.*, **19**, 1911 (1975).
4. A. J. Glass and A. H. Guenther, *Appl. Opt.*, **16**(5), 1214 (1977).
5. J. R. Hollahan, T. Wydeven, and C. Johnson, *Appl. Opt.*, **13**(8), 1844 (1974).
6. J. R. Hollahan and A. T. Bell, Eds., *Techniques and Applications of Plasma Chemistry*, Wiley, New York, 1974.
7. K. G. Donohoe, Ph.D. Thesis, California Institute of Technology, Pasadena, California, 1976.
8. K. G. Donohoe, O. R. Wulf, and F. H. Shair, *Ind. Eng. Chem., Fundam.*, **16**, 708 (1977).
9. H. Kobayashi, M. Shen, and A. T. Bell, *J. Macromol. Sci. Chem. A*, 8(2), 373 (1974).
10. H. Kobayashi, A. T. Bell, and M. Shen, *J. Appl. Polym. Sci.*, **17**, 885 (1973).
11. J. E. Lovelock, *Anal. Chem.*, **33**, 162 (1961).
12. W. H. Bennett, *Phys. Rev.*, **45**, 890 (1934).
13. M. Hudis and T. Wydeven, *J. Polym. Sci., Polym. Lett. Ed.*, **13**(9), 549 (1975).
14. H. Kobayashi, M. Shen, and A. T. Bell, *Macromolecules*, **7**(3), 277 (1974).
15. L. F. Thompson and G. Smolinsky, *J. Appl. Polym. Sci.*, **16**, 1179 (1972).
16. P. Beckmann and A. Spizzichino, *The Scattering of Electronmagnetic Waves from Rough Surfaces*, Macmillan, New York, 1973.
17. R. D. Cadle, *Particle Size*, Reinhold, New York, 1965, Chap. 2.

Received March 31, 1978
Revised June 30, 1978